Demystifying Orbital Emergencies: A Pictorial Review[1]

Viet D. Nguyen, MD
Achint K. Singh, MD
Wilson B. Altmeyer, MD
Bundhit Tantiwongkosi, MD

Abbreviations: CN = cranial nerve, FLAIR = fluid-attenuated inversion-recovery, IgG4 = immunoglobulin G4, IOFB = intraorbital foreign body, MRSA = methicillin-resistant *Staphylococcus aureus*

RadioGraphics 2017; 37:947–962

Published online 10.1148/rg.2017160119

Content Codes: CT ER HN MR

[1]From the Department of Radiology, University of Texas Health Science Center at San Antonio, 7703 Floyd Curl Dr, MC 7800, San Antonio, TX 78229. Recipient of a Magna Cum Laude award for an education exhibit at the 2015 RSNA Annual Meeting. Received April 24, 2016; revision requested October 20 and received November 14; accepted January 10, 2017. For this journal-based SA-CME activity, the authors, editor, and reviewers have disclosed no relevant relationships. **Address correspondence to** V.D.N. (e-mail: *vietng@gmail.com*).

SA-CME LEARNING OBJECTIVES

After completing this journal-based SA-CME activity, participants will be able to:

- Identify the relevant imaging anatomy of the orbit.
- Recognize the role of imaging modalities in orbital emergencies and select appropriate imaging protocols.
- Apply a systematic approach to the radiologic characterization of orbital emergencies.

See www.rsna.org/education/search/RG.

Imaging of the orbit plays an important role in the workup of orbital emergencies. Orbital imaging is particularly useful in the emergency department, where clinical history and physical examination may be limited or delayed until the exclusion or treatment of more life-threatening conditions. Cross-sectional orbital imaging with multidetector computed tomography (CT) and magnetic resonance (MR) imaging is commonly performed in addition to ultrasonography. In an emergent setting, CT is the preferred modality when evaluating for intraorbital foreign bodies, fractures, or calcifications within a mass lesion. MR imaging is typically the modality of choice for orbital pathologic conditions, owing to its superior ability to delineate the orbital soft tissues and visual pathways. CT and MR imaging together may supplement clinical evaluation by helping establish an accurate diagnosis, providing an objective assessment of disease extent and progression, and assisting in pretreatment planning. Orbital emergencies have a spectrum of cross-sectional imaging findings in four major categories: infection, trauma, vascular disease, and inflammation. Use of a systematic approach to these entities will assist the radiologist with identifying immediate threats to vision and thereby facilitate prompt clinical management. Familiarity with the clinical presentations also improves the radiologist's diagnostic confidence and role in guiding patient care. This article reviews imaging protocols, relevant orbital anatomy, the role of CT and MR imaging, and key imaging findings of orbital emergencies that the radiologist must know.

Introduction

Orbital emergencies accounted for more than 40% of the 11.9 million eye-related visits to the emergency department in the United States from 2006 to 2011 (1). Orbital emergencies exhibit a spectrum of imaging findings that help guide the clinician to specific treatment regimens and predict distinct clinical outcomes. There are four major categories from which orbital emergencies can arise: infection, trauma, vascular disease, and inflammation. Recognizing the category that a presenting entity belongs to can help guide the differential diagnosis. Additional consideration should be given to the various orbital compartments from which each entity arises. Radiologic evaluation of the orbit is especially crucial when clinical evaluation is limited by the patient's inability to cooperate, extensive facial trauma, or more life-threatening injuries elsewhere in the body. This article reviews imaging protocols, relevant orbital anatomy, the

TEACHING POINTS

- The paranasal sinuses, especially the ethmoid sinuses, are the main source of orbital infection. Therefore, orbital cellulitis may manifest as the first sign of acute to subacute sinusitis in children.
- Intraocular hemorrhage in a child is highly specific (up to 95% specificity) for nonaccidental trauma. The need for an additional search for subarachnoid or subdural hemorrhages and skull fractures with use of nonenhanced head CT should be conveyed to the clinician.
- Bilateral or spontaneous lens dislocations or those occurring after minor trauma, especially in a child, should prompt further evaluation for systemic conditions such as Marfan syndrome, Ehlers-Danlos syndrome, homocystinuria, sulfite oxidase deficiency, and Weill-Marchesani syndrome.
- Contrast-enhanced MR imaging of the spine is also indicated in rare cases of a spinal mass causing increased intracranial pressure without symptoms of neck or back pain or myelopathy.
- Postinfectious causes of optic neuropathy should be considered as alternatives to optic neuritis in the pediatric population, while ischemic optic neuropathy (eg, due to vasculopathic risk factors or giant cell arteritis) is a more likely diagnosis than optic neuritis in patients older than 50 years.

role of computed tomography (CT) and magnetic resonance (MR) imaging, and key imaging findings of orbital emergencies that the radiologist must know.

Imaging Protocols

Cross-sectional imaging plays an important role in extending the characterization of orbital emergencies beyond funduscopy (ophthalmoscopy). Ocular ultrasonography (US) is useful for evaluating the globe and its contents; however, it is operator dependent and is generally contraindicated if there is a possibility of a ruptured globe. The applied pressure from the transducer may elevate intraocular pressure and worsen the extrusion of vitreous humor from a ruptured globe (2,3). MR imaging is typically the modality of choice for orbital disease because of its superior ability to delineate the orbital soft tissues and visual pathways. In an emergent setting, multidetector CT is often the first-line imaging modality, particularly when evaluating for intraorbital foreign bodies (IOFBs), fractures, or calcifications within a mass lesion. It is important to consider the presence and type of foreign body a patient may have in the setting of trauma, as MR imaging is contraindicated with suspected ferromagnetic IOFBs. Nevertheless, CT and MR imaging are complementary modalities, supplementing clinical evaluation by helping establish an accurate diagnosis, providing an objective assessment of disease extent and progression, and assisting in pretreatment planning (4). Unless contraindicated, intravenous contrast media should be administered in the setting of inflammation, infection, neoplasm, or vascular malformation (Table 1) (5).

Anatomic Considerations

The orbit is a pyramidal socket of the skull that is formed by the frontal, sphenoid, ethmoid, lacrimal, zygomatic, and palatine bones and the maxilla (5). The orbital contents are divided into compartments comprising the globe, muscle cone, intraconal space, and extraconal soft tissues (Fig 1a). Located at the orbital base or anterior orbit, the globe wall consists of three distinct layers: the sclera, uvea, and retina. The uvea is composed of the choroid, iris, and ciliary body. The uvea shows enhancement on contrast material–enhanced T1-weighted images as compared with the retina and sclera (6) (Fig 1b). Attached to the sclera by zonular fibers, the lens separates the globe into an anterior segment containing aqueous humor and a posterior segment containing vitreous humor. The anterior segment is divided by the iris into anterior and posterior chambers. The muscle cone, comprising six extraocular muscles that control eye movement, forms a tendinous ring called the annulus of Zinn at its convergence at the orbital apex. The muscle cone separates the intraconal and extraconal contents.

Several important structures pass through the annulus of Zinn, including the optic nerve (cranial nerve [CN] II) and ophthalmic artery contained within the optic nerve sheath, the oculomotor nerve (CN III), the abducent nerve (CN VI), and the nasociliary branch of the ophthalmic nerve (CN V1). The optic nerve, a bundle of more than 1 million retinal ganglion cell axons, is an extension of the central nervous system. The optic nerve is surrounded by cerebrospinal fluid and meninges: the pia mater, arachnoid membrane, and dura (7) (Fig 1c). The orbit is connected to the intracranial structures via the optic canal (CN II), superior orbital fissure (CNs III, IV, V1, and VI), and inferior orbital fissure (CN V2).

Infection

Infections of the orbit account for more than half of primary orbital abnormalities; about two-thirds of the cases are secondary to sinusitis, while one-fourth are due to IOFBs (5). Emergent radiologic evaluation of orbital infections is commonly performed to distinguish anterior periorbital (preseptal) cellulitis from posterior deep (orbital) cellulitis with respect to the orbital septum. Although not well delineated at MR imaging or CT, the orbital septum is a fibrous membrane that extends from the periosteum of the orbit to the tarsal plates of the eyelids behind the orbicularis oculi muscles, and its location can be approximated by an imaginary line crossing

Table 1: Imaging Protocols for Orbital Imaging

Modality and Protocols	Special Cases
MR imaging (1.5 T or 3 T)	
Images acquired from the top of the frontal sinus to the hard palate Sequences: T1-weighted 3-mm axial and 3-mm coronal sections Fat-saturated T2-weighted 3-mm axial and 3-mm coronal sections Diffusion-weighted imaging with apparent diffusion coefficient mapping Contrast-enhanced fat-saturated T1-weighted 3-mm axial, coronal oblique (perpendicular to CN II), and sagittal oblique (parallel to CN II) sections Intravenous hand injection of gadolinium-based contrast agent; volume determined by patient weight (0.1 mL/kg)	Diffusion-weighted sequence: abscess, acute ischemic optic neuropathy Brain MR imaging with and without contrast material: intracranial extension of orbital diseases, optic neuritis with multiple sclerosis MR venography: papilledema, superior opthalmic vein thrombosis
Multidetector CT	
Acquired helically from top of frontal sinus to hard palate Iterative reconstruction in soft tissue and bone kernels on coronal oblique (perpendicular to CN II) and sagittal oblique (parallel to CN II) views Parameters: 120 kVp, 100 mAs, 1.25-mm section thickness with 1.25-mm intervals Intravenous hand injection of iodinated contrast material (70 mL, 2 mL/sec)	CT angiography: evaluation of vascular lesions (eg, carotid cavernous fistulas or aneurysms)

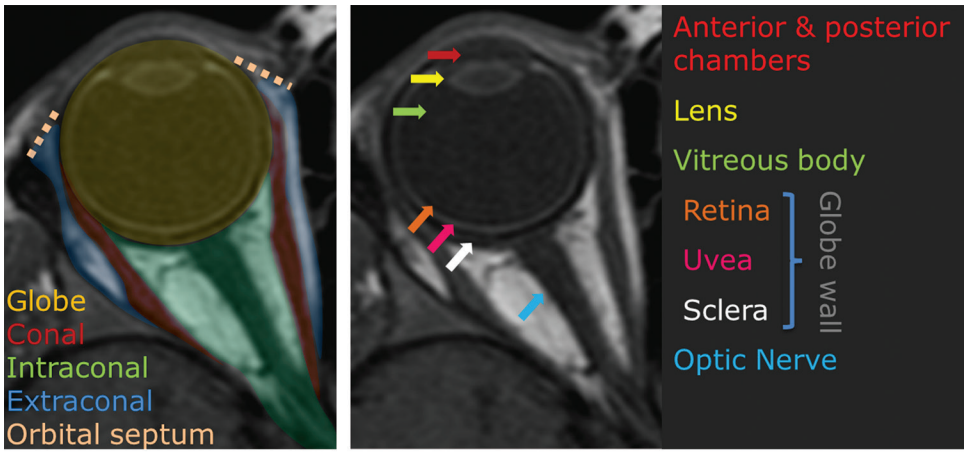

a. b.

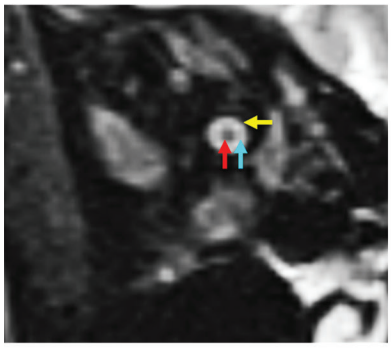

c.

Figure 1. Normal ocular anatomy. **(a, b)** Axial contrast-enhanced T1-weighted orbital MR images show the orbit **(a)** and globe **(b)**. The dotted lines in **a** indicate the expected location of the orbital septum, which separates the preseptal and postseptal spaces. **(c)** Coronal T2-weighted orbital MR image shows the components of the optic nerve sheath, which include CN II and the pia mater (red arrow), cerebrospinal fluid (blue arrow), and the arachnoid mater and dura (yellow arrow).

the anterior globe and connecting the orbital rim (Fig 1a). The orbital septum serves as a natural barrier against the spread of infection (8). Therefore, the location of an orbital infection has profound clinical implications, with deep orbital infection requiring more aggressive treatment to prevent vision loss and intracranial spread.

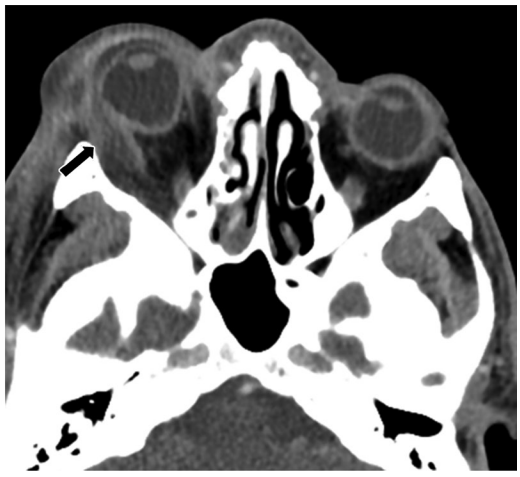

a.

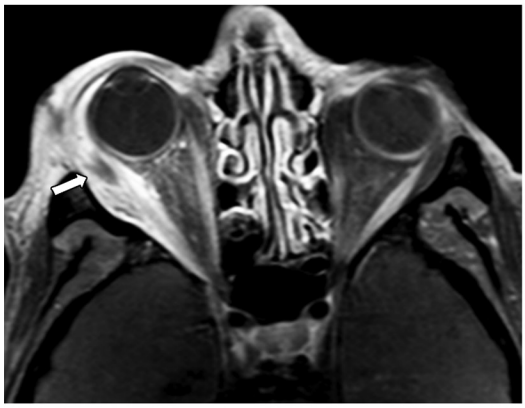

b.

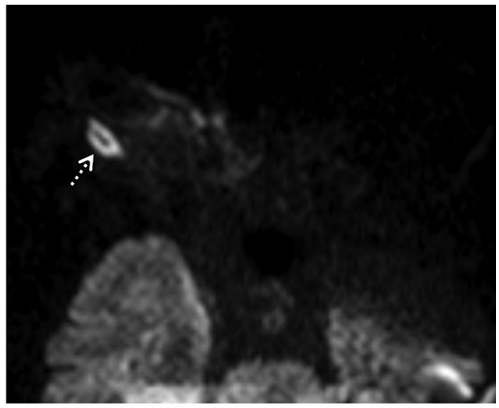

c.

Figure 2. Intraorbital abscess in a 45-year-old woman. **(a)** Axial contrast-enhanced CT image of the orbits reveals right proptosis with globe deformity (the "guitar pick" sign) and periorbital edema with a rim-enhancing fluid collection (arrow) in the right lateral extraconal space. **(b)** Axial contrast-enhanced T1-weighted MR image shows the rim-enhancing fluid collection (arrow) abutting and displacing the right lateral rectus muscle. **(c)** Axial diffusion-weighted MR image shows restricted diffusion (arrow).

Orbital and Subperiosteal Abscess

Preseptal cellulitis and orbital cellulitis are commonly encountered in the pediatric population. While both may cause eyelid edema and erythema, they have different imaging features and clinical implications. On cross-sectional images, preseptal cellulitis is characterized by periorbital soft-tissue swelling and stranding anterior to the orbital septum. It is commonly caused by the contiguous spread of infection from adjacent structures such as the face, tooth, and eyelid or by direct inoculation from local trauma or insect bites (8). The clinical course of preseptal cellulitis typically ends with outpatient antibiotic treatment and rarely involves serious complications.

In contrast, orbital cellulitis is a postseptal soft-tissue infection that involves the contents of the orbit, with threat to vision. It generally requires hospital admission with administration of intravenous antibiotics and close monitoring of the patient's vision. The paranasal sinuses, especially the ethmoid sinuses, are the main source of orbital infection (8,9). Therefore, orbital cellulitis may manifest as the first sign of acute to subacute sinusitis in children (5). Orbital cellulitis typically shows diffuse soft-tissue stranding posterior to the orbital septum and clinical features of proptosis (exophthalmos), painful ophthalmoplegia, and vision loss. One of the serious complications of orbital cellulitis is orbital abscess. An orbital abscess typically manifests as a peripherally enhancing fluid collection (Fig 2a, 2b), with central restricted diffusion seen at diffusion-weighted MR imaging (Fig 2c). Likewise, acute ethmoid sinusitis is the most common cause of orbital subperiosteal abscess in children (10) (Fig 3). A subperiosteal abscess is characterized as a lenticular rim-enhancing fluid collection along the orbital wall with adjacent sinusitis.

Invasive Fungal Infection

Most cases of orbital cellulitis are bacterial in origin. Orbital infections are occasionally caused by invasive fungal pathogens, particularly Mucorales and *Aspergillus* species. These invasive fungi are particularly aggressive and life threatening (5). Affecting primarily immunocompromised patients and those with diabetes, the infection starts with inhalation of the fungal spores into the paranasal sinuses, which leads to invasion of the vasculature by fungal hyphae and to eventual necrosis of the infected tissues (11). Orbital ex-

Figure 3. Subperiosteal abscess due to ethmoid sinusitis in a 14-year-old male adolescent. Axial contrast-enhanced CT image through the orbits shows a left subperiosteal abscess (solid black arrow) extending into the medial extraconal orbit and causing displacement of the medial rectus. Note the adjacent left ethmoid sinusitis (dotted black arrow). Periorbital edema is also evident (white arrow).

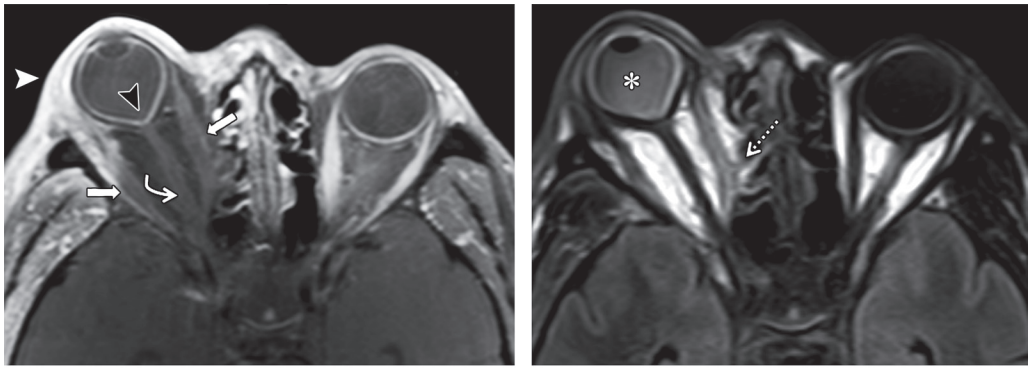

a. **b.**

Figure 4. Mucormycosis in a 52-year-old man with poorly controlled diabetes. **(a)** Axial contrast-enhanced fat-saturated T1-weighted MR image of the orbits shows nonenhancing right medial and lateral rectus muscles (straight arrows), severe proptosis, periorbital edema (white arrowhead), tenting of the posterior globe ("guitar pick" sign) (black arrowhead), and stretching of the optic nerve (curved arrow). **(b)** Axial fluid-attenuated inversion-recovery (FLAIR) MR image shows increased signal intensity in the right vitreous body (*), a finding that represents intraocular invasion. Note the emergent right medial orbital wall decompression (arrow). The cause was adjacent acute right maxillary fungal sinusitis (not shown).

tension typically manifests as periorbital swelling, inflammation, and proptosis. When proptosis is severe, the dorsal globe becomes deformed and demonstrates the "guitar pick" sign (Fig 4a). The mixture of necrosis and inflammation results in a variable enhancement pattern. Treatment includes a combination of aggressive surgical débridement, intravenous antifungal therapy, and correction of the underlying immunodeficiency. Increased mortality rates are seen in patients with cerebral extension of infection (12).

Endophthalmitis

Endophthalmitis is defined as a bacterial or fungal infection within the globe that involves the vitreous or aqueous humor. Most cases of endophthalmitis are exogenous and are due to direct inoculation of organisms into the globe from trauma or ocular surgery or are an extension of corneal infection that seeds the aqueous humor before spreading into the vitreous humor (13). Less commonly, endogenous endophthalmitis (Fig 5) is due to organisms that seed the highly vascular choroid first before extending into the vitreous humor. Cross-sectional imaging findings of endophthalmitis are periocular inflammation, thickening and enhancement of the ocular wall, hyperattenuation at CT, and abnormal increased signal intensity on FLAIR MR images of the affected vitreous humor. Acute bacterial endophthalmitis is a vision-threatening emergency, with the clinical outcome dependent on expedited diagnosis and initiation of treatment that includes intravitreal antibiotic injections and vitrectomy in severe cases.

Orbital Compartment Syndrome

Orbital compartment syndrome (OCS) is a serious ophthalmologic emergency. Because the orbit is confined by its surrounding bone walls, acute intraorbital pressure elevation may result in impaired perfusion and ischemia of the optic nerve and globe. While posttraumatic retrobulbar hemorrhage is the most common cause of OCS, it can also occur after infection, inflammation, emphysema (tension pneumo-orbitus), or periocular or sinus surgery (14). Symptoms include decreased visual acuity, marked proptosis, and evidence of increased intraorbital pressure. OCS is primarily

Figure 5. Acute endogenous endophthalmitis in a 54-year-old woman with diabetes, methicillin-resistant *Staphylococcus aureus* (MRSA) bacteremia, and abrupt left-sided vision loss. Axial contrast-enhanced fat-saturated T1-weighted MR image of the left orbit shows periocular inflammation (arrowhead) and thickening and enhancement of the ocular wall that involves the episclera (dotted arrow) and choroid (solid arrow).

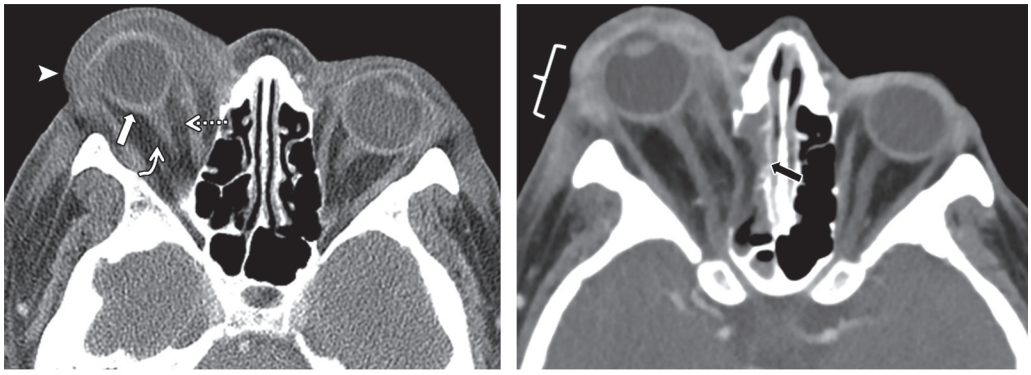

a. **b.**

Figure 6. Orbital compartment syndrome due to MRSA orbital cellulitis in a 50-year-old woman with uncontrolled type II diabetes. **(a)** Axial contrast-enhanced CT image of the right orbit shows severe proptosis, periorbital edema (arrowhead), retrobulbar stranding (dotted arrow), tenting of the posterior globe (solid straight arrow), and stretching of the optic nerve (curved arrow). The patient underwent right lateral canthotomy, endoscopic medial orbital wall decompression, and orbital access drainage. **(b)** Axial orbital contrast-enhanced CT image obtained after surgery shows changes related to the right lateral canthotomy (bracket), endoscopic medial orbital wall decompression (arrow), and orbital abscess drainage.

a clinical diagnosis, and emergent intervention is needed because only 60–100 minutes of elevated pressure can cause permanent vision loss (14). At imaging, OCS will manifest as severe proptosis with tenting of the posterior globe and stretching of the optic nerve (Fig 6a). Management of OCS includes emergent lateral canthotomy and inferior cantholysis to decompress the orbit (Fig 6b).

Trauma

Retinal and Choroidal Hemorrhages

Traumatic injury to the globe may result in several different intraocular hemorrhage and detachment patterns that are distinguishable at cross-sectional imaging. Hyphema appears as layering hemorrhage or hyperattenuation within the anterior chamber on nonenhanced CT images. Although hyphema is grossly apparent at clinical examination, it should prompt a search for additional intraocular injuries at cross-sectional imaging because these may be obscured by the anterior chamber hemorrhage at clinical inspection. Retinal detachment or hemorrhage occurs after a full-thickness retinal break between the retinal pigment epithelium and sensory retinal layers. It has a characteristic *V*-shaped appearance on axial images, with the apex at the optic disk margin and the base at the ora serrata retinae (junction of the retina and ciliary body) (Fig 7). On the other hand, choroidal detachment or hemorrhage has a lentiform or biconvex shape, sparing the optic disk and posterior third of the globe and extending anteriorly to the ciliary body beyond the ora serrata retinae (Fig 8). Recognition of these injuries is important not only for timely management but also for detection of the underlying cause, such as an intraocular neoplasm or nonaccidental trauma. Intraocular hemorrhage in a child is highly specific (up to 95% specificity) for nonaccidental trauma (15). The need for an additional search for subarachnoid or subdural hemorrhages and skull fractures with use of nonenhanced head CT should be conveyed to the clinician.

Open Globe Injury

Open globe injury refers to a traumatic breakdown in the sclera or cornea of the eye after blunt

Figure 7. Hemorrhagic retinal detachment in a 47-year-old male inmate. Axial nonenhanced CT image of the left orbit shows a classic *V*-shaped retinal detachment with hemorrhage (arrows), with the apex at the optic disk.

Figure 8. Hemorrhagic choroidal detachment and lens subluxation in a 37-year-old man. Axial CT image of the orbits shows a hyperattenuating lentiform hemorrhage (dotted arrows) along the medial and lateral ocular walls that spares the optic disk and posterior third of the globe and extends anteriorly to the ciliary body beyond the ora serrata retinae. Note the abnormal angulation of the lens (solid arrow), a finding compatible with lens subluxation.

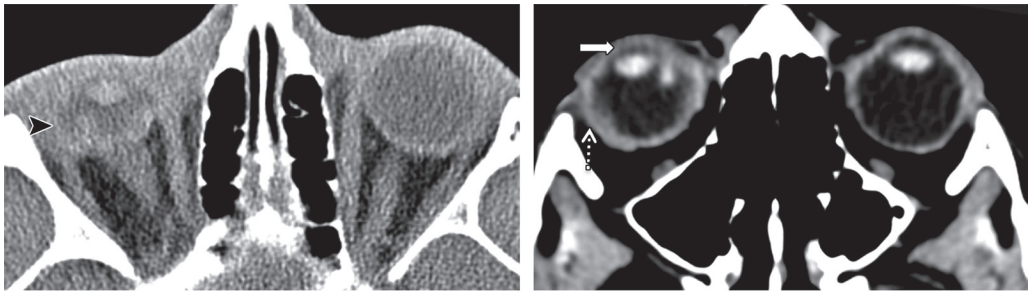

a. **b.**

Figure 9. Globe rupture in two patients. **(a)** Axial nonenhanced CT image of the orbits in a 26-year-old man shows a collapsed right globe (arrowhead) with an irregular folded posterior contour and loss of the majority of the vitreous body. The patient underwent emergent repair of the right globe and of facial lacerations (not shown). **(b)** Axial nonenhanced CT image in a 33-year-old man with open globe injury shows a shallow anterior segment (solid arrow), globe volume loss, and intravitreous hemorrhage (dotted arrow).

or penetrating injury. Open globe rupture due to blunt trauma commonly occurs at the site of greatest structural weakness, near the insertion of the extraocular muscles or along the equator. Open globe laceration occurs after a penetrating injury to the eye and is further characterized as penetrating (entry wound without exit wound) or perforating (both entry and exit wounds). These injuries are typically complicated by an intraocular foreign body. CT is the modality of choice for assessing suspected open globe injuries, as it is superior to US for evaluating the location and size of IOFBs. Compared with MR imaging, CT will not cause movement of metallic IOFBs and is less time consuming in a critically ill patient. Findings of open globe injuries at CT include globe deformity and volume loss ("flat tire" sign), decreased or increased anterior chamber depth, IOFBs, and intraocular air (Fig 9) (5,16). Furthermore, any alteration of the normal mean anterior chamber depth of 3.1 mm that is 0.8 mm or greater when compared with the contralateral eye is diagnostic for globe rupture (17). Depending on the segment that has lost volume, the anterior chamber depth may decrease or increase after injury to the anterior or posterior segment, respectively (5,16,18). In patients with multiple injuries and a likelihood of open globe injury, the clinician will focus on more life-threatening injuries and avoid any examination that might apply pressure to the globe. Therefore, prompt recognition of an open globe injury at imaging and emergent ophthalmologic consultation are essential for optimal restoration of vision.

Lens Dislocation

Lens dislocation (ectopia lentis) may occur after blunt trauma or secondary to an underlying ocular or systemic disease. It is described as subluxation when the partially dislocated lens remains attached to the ciliary body and as luxation when the lens is completely detached. Traumatic lens dislocation typically occurs in association with other orbital injuries, such as ruptured globe, intraocular hemorrhage, and orbital fractures. Bilateral or spontaneous lens dislocations or those occurring after

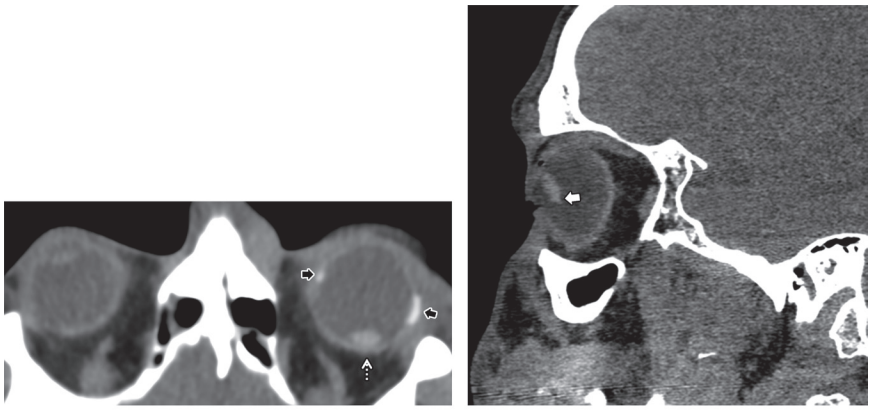

a. b.

Figure 10. Traumatic posterior lens luxation and subluxation. **(a)** Axial CT image of the orbits in a 28-year-old woman shows posterior lens luxation, with the left lens in the posterior segment (white arrow). The patient also had left orbital fractures (not shown) and radiopaque scleral buckle (black arrows) from prior retinal detachment treatment. **(b)** Sagittal nonenhanced CT image in a 19-year-old man shows posterior lens subluxation, with the inferior aspect of the lens posteriorly displaced because of a tear of the zonular fibers (arrow), while the location of the superior margin remains normal.

Figure 11. Traumatic cataract in a 21-year-old man. Axial nonenhanced CT image of the orbits shows the right lens (arrow) with an indistinct margin and decreased attenuation relative to the contralateral unaffected lens.

minor trauma, especially in a child, should prompt further evaluation for systemic conditions such as Marfan syndrome, Ehlers-Danlos syndrome, homocystinuria, sulfite oxidase deficiency, and Weill-Marchesani syndrome (19). Cross-sectional imaging will demonstrate abnormal positioning of the lens, which is often displaced posteriorly (Fig 10a). While anterior lens dislocation is less common because of the presence of the iris (20), it may manifest as decreased anterior chamber depth at imaging and is difficult to differentiate from volume loss due to anterior chamber open globe injury. The clinician should be alerted if there is suspicion for anterior lens dislocation because it may induce acute angle-closure glaucoma, which is a surgical emergency (20). When the lens is within its expected location, any subtle angulation of the lens relative to its zonular attachments may suggest lens subluxation (Figs 8, 10b). Careful evaluation of the lens position in three planes is crucial in detecting subtle lens subluxation. Treatment of lens dislocation may include correction of the refractive error, lensectomy/vitrectomy, or intraocular lens placement, depending on the extent, cause, and associated disorders.

Traumatic Cataract

Traumatic cataract occurs after blunt or penetrating injury to the eye with disruption of the lens capsule. CT will demonstrate decreased attenuation of the edematous affected lens relative to the contralateral unaffected lens (Fig 11) (5). The decreased attenuation is secondary to increased fluid that dilutes the normally high protein content within the lens, and it corresponds to acute cataract formation seen at physical examination (5,21). Although traumatic cataract is easily recognized at clinical examination, CT is helpful in identifying other intraocular injuries that may be obscured clinically by the lens opacification. In complicated orbital injuries that preclude clinical evaluation, CT may be useful for diagnosing unsuspected lens injury (21). Management of traumatic cataract varies with the age of the patient, especially because there is potential for interference with visual development in a child.

Traumatic Optic Neuropathy

Traumatic optic neuropathy (TON) is seen in up to 5% of patients who present with closed-head trauma in the United States (22). It is primarily a clinical diagnosis characterized by loss of vision without initial funduscopic findings of optic nerve head abnormality in a patient after blunt or penetrating trauma. TON is classified as direct or indirect type. Direct TON occurs when there is direct injury to the optic nerve that results in disruption of the nerve (Fig 12). The more common

Figure 12. Traumatic optic neuropathy in a 43-year-old man who sustained a gunshot injury. Axial contrast-enhanced CT image shows a severed right posterior intraorbital optic nerve (solid arrow), with soft-tissue attenuation in the orbital apex representing edema and hematoma. Bone and ballistic fragments are scattered along the bullet track (dotted arrows).

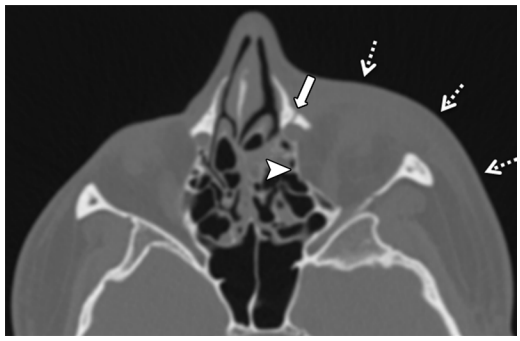

Figure 13. Lacrimal bone fracture in a 17-year-old woman. Axial nonenhanced CT image shows a nondisplaced left lacrimal bone fracture (solid arrow) extending to the medial orbital wall (arrowhead). There is partially demonstrated left periorbital soft-tissue edema (dotted arrows).

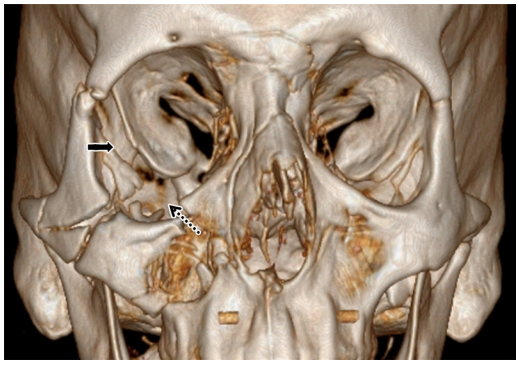

Figure 14. Increased orbital volume in a 61-year-old man. Three-dimensional surface volume-rendered CT image of the orbits shows displaced right orbital floor (dotted arrow) and lateral orbital wall (solid arrow) fractures, with widening of the fractures resulting in increased orbital volume. There is increased risk for enophthalmos, which may develop after the orbital edema subsides.

indirect type occurs when blunt force from the site of impact is transmitted to the intracanalicular optic nerve within the optic canal. There is no obvious optic canal fracture. CT is the modality of choice to depict IOFBs, fractures, and intraorbital hemorrhages. Increased attenuation in the fat about the intracanalicular optic nerve in the setting of orbital fracture is suspicious for optic nerve injury. MR imaging demonstrates the optic nerve with T2 hyperintensity ipsilateral to the origin of the trauma (22,23). The management of TON remains controversial; no specific treatment (including surgery) in the literature to date has been shown to be superior to observation (24,25).

Orbital Fractures and Foreign Bodies

Orbital fractures are often a component of complex facial trauma and have been described extensively in the literature. They include Le Fort II fractures involving the medial wall and orbital floor; Le Fort III fractures involving the medial and lateral orbital walls; naso-orbitoethmoid (NOE) complex fractures involving the medial orbital wall and often the attachment site of the medial canthal tendon; zygomaticomaxillary complex (ZMC) fractures involving the orbital floor and lateral wall; and orbital blow-out fractures (26). Because of comminution of the medial orbital wall, one possible complication of NOE fractures is traumatic telecanthus from a medial canthal tendon injury. Furthermore, trauma to the medial orbit may injure the nasolacrimal drainage apparatus (Fig 13), leading to epiphora (27). ZMC and orbital blow-out fractures may lead to enophthalmos due to increased orbital volume (Fig 14). The measurement of orbital volume at CT has been shown to correlate well with the degree of enophthalmos and therefore allows early surgical intervention (28). In addition, CT is useful for evaluating extraocular muscle entrapment related to blow-out fracture.

Identification of IOFBs is important in the evaluation of orbital emergencies. CT is the preferred imaging modality when IOFBs are suspected (Fig 12) (3,16). Because of several limitations, MR imaging and US are reserved as adjunct examinations in the case of equivocal or negative CT findings. Special attention is needed to assess for wooden foreign bodies, which carry high risk for endophthalmitis (3). The attenuation of wood at CT imaging is lower than that of surrounding vitreous, and wood can be mistaken for air. Measuring the attenuation in Hounsfield units may aid in differentiating the types of foreign bodies, especially wood (−100 to −200 HU initially and increasing in attenuation over time because of fluid accumulation) versus air (−1000 HU) (29). It is suggested that T2-weighted or contrast-enhanced MR imaging performed with fat suppression can depict the inflammatory

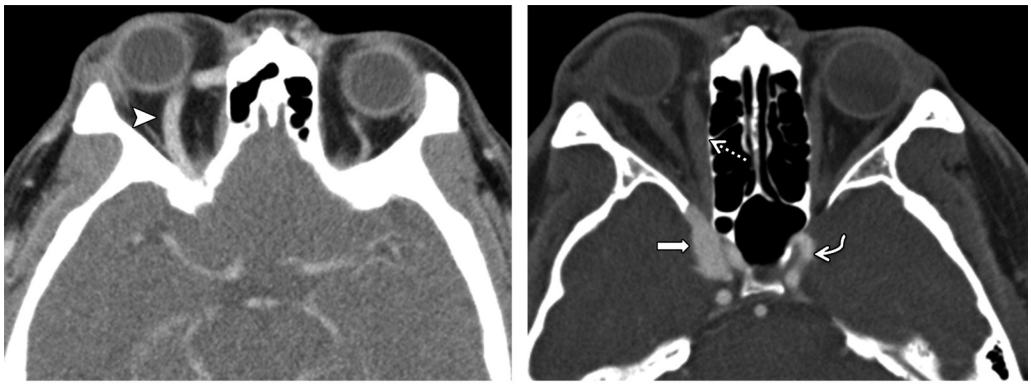

a. b.

Figure 15. Carotid cavernous fistula in a 47-year-old man with a history of motor vehicle collision who developed progressive right vision loss and proptosis. Axial contrast-enhanced CT images in soft-tissue **(a)** and vascular **(b)** windows show early enhancement of the dilated right superior ophthalmic vein (arrowhead in **a**) and cavernous sinus (solid straight arrow in **b**), with attenuation similar to that of the internal carotid artery (curved arrow in **b**). Note the right extraocular muscle enlargement (dotted arrow in **b**) and proptosis.

response surrounding a nonferromagnetic IOFB (16). It is also helpful for the radiologist to be familiar with mimics of IOFBs, such as scleral buckle (Fig 10a).

Vascular Conditions

Carotid Cavernous Fistula

Carotid cavernous fistulas (CCFs) are acquired abnormal communications between the carotid artery and the cavernous sinus. CCFs may be secondary to head trauma, ruptured aneurysm, dural venous sinus thrombosis, or an underlying genetic vasculopathy (eg, fibromuscular dysplasia, Ehlers-Danlos syndrome, or pseudoxanthoma elasticum) (5). In many cases, a cause is not identified. CCFs are primarily classified as a direct high-flow shunt (type A) between the intracavernous carotid artery and the cavernous sinus, or an indirect low-flow/dural shunt between the cavernous sinus and branches of the internal (type B), external (type C), or both internal and external (type D) carotid arteries within the adjacent dura (30). Patients with direct CCFs may present with abrupt onset of bruit, pulsatile proptosis, conjunctival injection, ophthalmoplegia, pain, or progressive vision loss. Indirect or dural CCFs typically have a more subacute and mild manifestation. Imaging findings that suggest a diagnosis of CCF include ipsilateral proptosis, enlargement of the superior ophthalmic vein, edematous intraorbital fat, enlargement of the extraocular muscles, and early enhancement of the cavernous sinus (Fig 15) (5). Digital subtraction angiography allows dynamic evaluation of blood flow through the cavernous sinuses and helps optimize endovascular treatment. Emergent closure of the CCFs is typically reserved for patients at risk for intracranial hemorrhage, progressive vision loss, ophthalmoplegia, or elevated intraocular pressure or is based on high-risk angiographic features (eg, pseudoaneurysm, large varix of the cavernous sinus, or dangerous collateral pathways) (31).

Posterior Ischemic Optic Neuropathy

Posterior ischemic optic neuropathy (PION) is an acute infarction of the retrobulbar optic nerve, leading to abrupt painless monocular vision loss, typically in patients older than 50 years (32). It can be clinically distinguished from the more commonly encountered anterior ischemic optic neuropathy (affecting the optic nerve head) by a normal-appearing optic disk at funduscopy. Because of its superficial and poor vascular supply, the posterior segment of the optic nerve is particularly susceptible to ischemia, which leads to swelling and further optic nerve compression within the optic canal. Although more than half of PION cases are idiopathic, PION been described in the setting of giant cell arteritis and perioperative hypotension (32,33). Restricted diffusion may be seen in the affected nerve at MR imaging (Fig 16b). More importantly, MR imaging is performed to exclude other inflammatory, infiltrative, and compressive causes of optic neuropathies. Although significant recovery of vision in the affected eye is unlikely, emergent diagnosis and treatment with corticosteroids are essential to prevent vision loss in the other eye.

Papilledema

Papilledema refers to bilateral optic disk swelling associated with intracranial hypertension. It is usually discovered during funduscopic examination for the evaluation of positional headache, horizontal diplopia with abducent nerve palsy, or transient visual deficits. Emergent diagnostic evaluation with contrast-enhanced cross-sectional

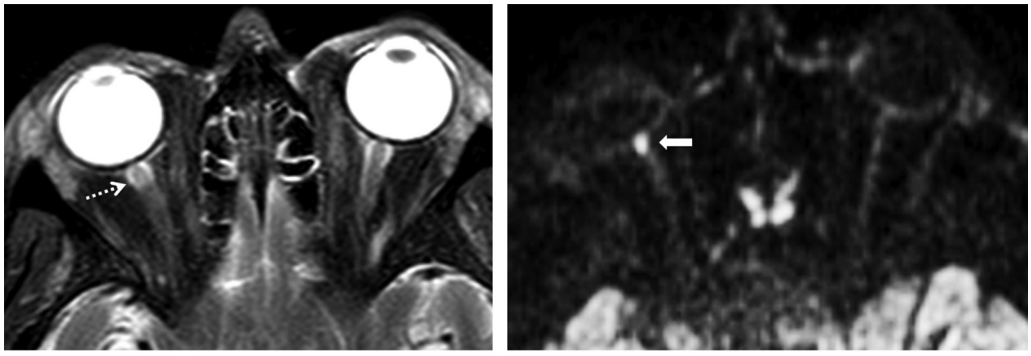

a. b.

Figure 16. Posterior ischemic optic neuropathy in a 50-year-old man with poorly controlled type II diabetes and peripheral vascular disease who developed sudden vision loss in his right eye after a left lower extremity amputation. The optic disk had a normal appearance at funduscopy. Axial T2-weighted **(a)** and diffusion-weighted **(b)** MR images show subtle T2 hyperintensity (arrow in **a**) with restricted diffusion (arrow in **b**) in the distal segment of the right intraorbital optic nerve.

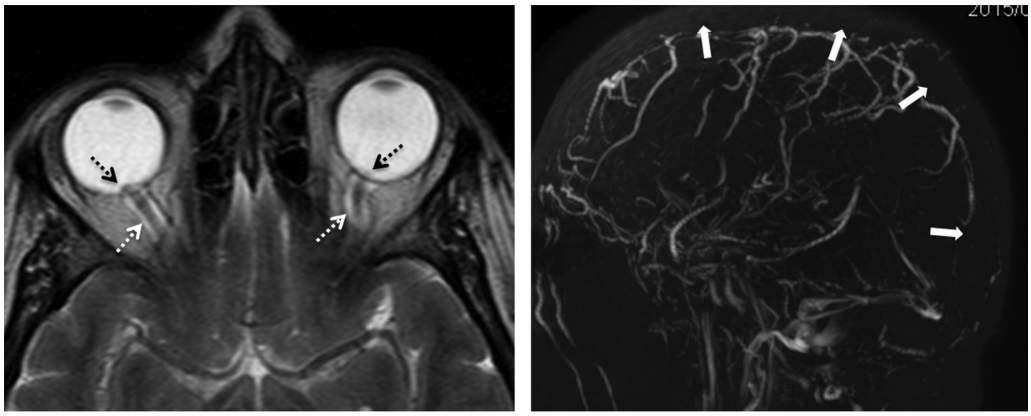

a. b.

Figure 17. Papilledema in a 16-year-old male adolescent. **(a)** Axial T2-weighted MR image shows bilateral protrusion of the optic disks (black arrows) into the posterior globes and increased cerebrospinal fluid within the optic nerve sheath (white arrows). **(b)** MR venogram shows superior sagittal sinus thrombosis (arrows), which is the cause of the intracranial hypertension and papilledema.

imaging is crucial to exclude causes of intracranial hypertension, such as space-occupying lesions, obstructive hydrocephalus, diffuse cerebral edema, and venous outflow obstruction. Contrast-enhanced MR imaging of the spine is also indicated in rare cases of a spinal mass causing increased intracranial pressure without symptoms of neck or back pain or myelopathy (34). It is suggested that imaging findings of papilledema lag behind the development of intracranial hypertension. Once intracranial hypertension is diagnosed, the severity of papilledema is commonly used as a measure of disease severity and treatment response (35). The cross-sectional imaging findings of papilledema are intraocular protrusion of the optic nerve heads, flattening of the posterior scleras, enlargement of the optic nerve sheaths, and tortuosity of the optic nerves (Fig 17a) (36). MR venography is typically performed concurrently to detect thrombosis in the dural venous sinuses and jugular veins (Fig 17b). If the neuroimaging findings are normal, a lumbar puncture is subsequently performed for opening pressure measurement and cerebrospinal fluid analysis. The treatment and prognosis of papilledema are dependent on the underlying cause of intracranial hypertension, and treatment is aimed at preventing blindness and permanent damage to the optic disks.

Superior Ophthalmic Vein Thrombosis

Superior ophthalmic vein thrombosis may occur in the setting of infection, inflammation, hypercoagulable states, or orbital mass lesion. It is most commonly secondary to orbital infection caused by paranasal sinusitis (5). Patients with superior ophthalmic vein thrombosis may present with orbital pain and swelling, decreased vision, chemosis, proptosis, and cranial nerve palsy. Superior ophthalmic vein thrombosis may progress to cavernous sinus thrombosis, or both conditions may occur at the same time with similar clinical

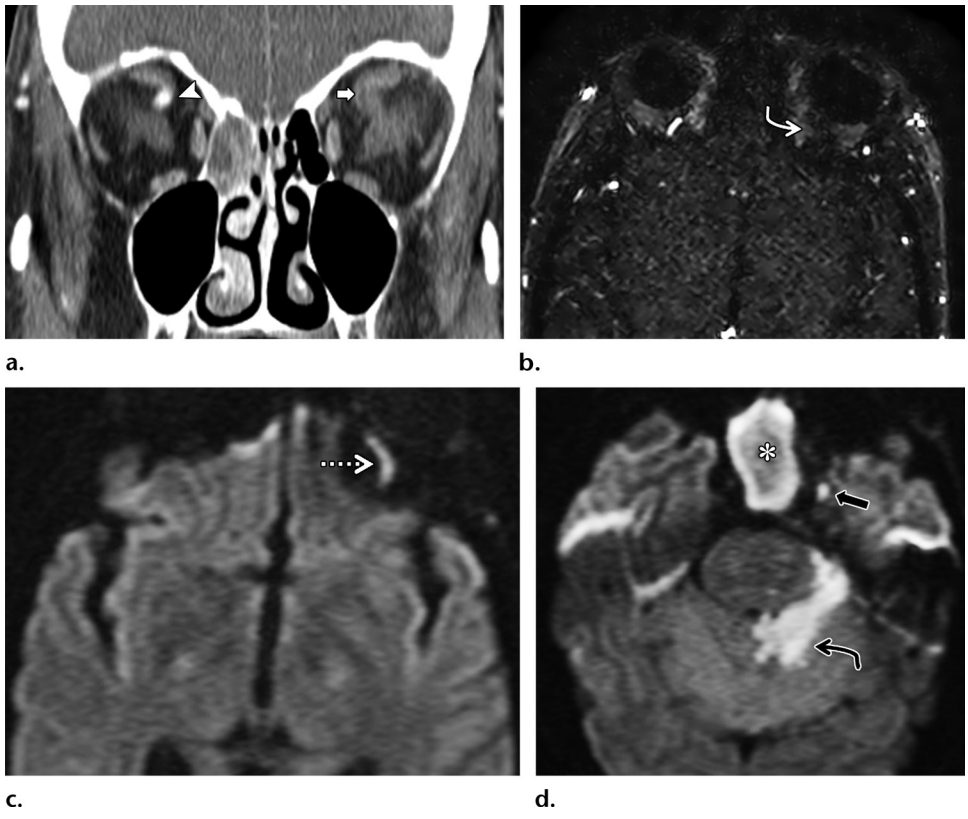

Figure 18. Superior ophthalmic vein thrombosis in a 46-year-old woman. **(a)** Coronal contrast-enhanced CT image shows a nonopacified dilated left superior ophthalmic vein (arrow). Arrowhead = right superior ophthalmic vein. **(b)** Axial MR venogram shows occlusion of the left superior ophthalmic vein (arrow). **(c, d)** Axial diffusion-weighted MR images (**c** obtained superior to **d**) show restricted diffusion in the left superior ophthalmic vein (arrow in **c**) and cavernous sinus thrombophlebitis with a small abscess (straight arrow in **d**). The pyomucocele (∗ in **d**) in the sphenoid sinuses is causing the thrombosis. Note the associated infarction of the left superior cerebellum (curved arrow in **d**). This case illustrates how infection of the orbit and paranasal sinuses can have rapid intracranial spread.

manifestations (37,38). Contrast-enhanced MR imaging and MR venography are more sensitive in the early stage of disease, which may be missed at CT. Imaging findings include a dilated nonopacified superior ophthalmic vein, often with associated enlargement of the cavernous sinus, congestion of the orbital soft tissues, and proptosis (Fig 18) (5,37). Treatment depends on the underlying cause and may consist of intravenous antibiotics, anticoagulation therapy, and possible surgical intervention with drainage of orbital abscess or sinus disease (37,38).

Inflammation

Orbital Pseudotumor

Orbital pseudotumor, also known as idiopathic orbital inflammatory syndrome, is a nongranulomatous inflammatory process of unknown etiology, accounting for approximately 10% of all orbital mass lesions (39). Patients classically present with acute to subacute unilateral orbital pain, cranial nerve palsies, diminished ocular motility, or decreased visual acuity. Contrast-enhanced MR imaging of the orbits demonstrates ill-defined masslike enhancing soft tissue involving any orbital compartment (Fig 19) (5). Bilateral involvement, which accounts for 25% of cases, is more common in children (39). Differential considerations include thyroid ophthalmopathy, lymphoma, granulomatosis with polyangiitis (Wegener granulomatosis), and orbital cellulitis (Table 2). The diagnosis is based on the patient's clinical course, laboratory tests, imaging findings, response to corticosteroid therapy, and exclusion of other causes. Biopsy is typically reserved for atypical presentations or refractory cases.

Immunoglobulin G4–related Orbital Disease and Tolosa-Hunt Syndrome

Immunoglobulin G4 (IgG4)–related orbital disease (IgG4-ROD) (Fig 20) and Tolosa-Hunt syndrome (THS) (Fig 21) are related to idiopathic orbital inflammatory syndrome, with almost identical clinical presentations and a dramatic response to corticosteroid therapy. Cross-sectional imaging shows similar findings with a different localization: idiopathic orbital

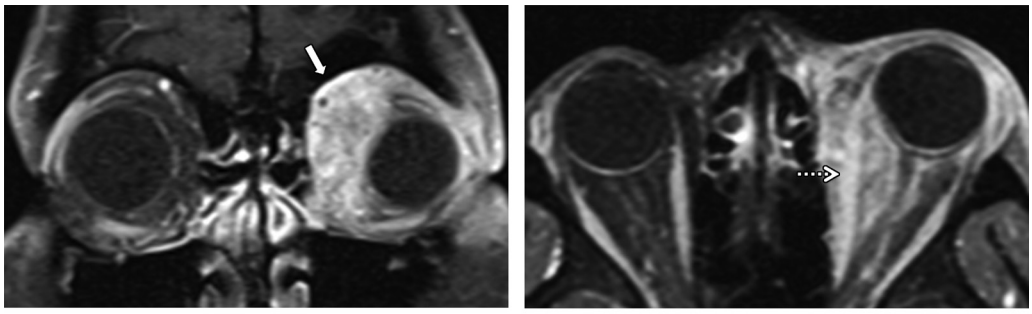

a. b.

Figure 19. Idiopathic orbital inflammatory syndrome, or orbital pseudotumor, in a 48-year-old woman. Coronal **(a)** and axial **(b)** contrast-enhanced T1-weighted MR images through the orbits show a poorly defined mass with heterogeneous enhancement (arrow in **a**) encasing the medial rectus muscle (arrow in **b**), with involvement of multiple orbital compartments. There is mild proptosis and lateral displacement of the globe.

Table 2: Characterization of Orbital Inflammatory Mimics

Condition	EOM Involvement	Lacrimal Gland Involvement	Signal Intensity at T2-weighted FSE and DW Imaging	Bilateral Involvement	Pain	Response to Steroid Therapy
Inflammatory pseudotumor	Superior and medial rectus muscles most commonly involved; may also involve their insertions	Yes	Often has areas of low T2-weighted FSE signal intensity due to fibrosis	25% of cases	Yes	Yes
Thyroid ophthalmopathy	Order of EOM involvement: inferior > medial superior > lateral; typically spares tendinous insertion EOMs	No	High T2-weighted FSE signal intensity in acute phase; low T2-weighted FSE signal intensity and presence of fat in chronic phase	90% of cases	Varies	Yes
Lymphoma (primary)	Random	Yes	Low T2-weighted FSE signal intensity with restricted diffusion	25% of cases	No	Can have transient response

Note.—DW = diffusion-weighted, EOM = extraocular muscle, FSE = fast spin-echo.

inflammatory syndrome remains intraorbital, THS extends to the cavernous sinus, and IgG4-ROD preferentially involves the lacrimal gland (IgG4-related dacryoadenitis). Imaging reveals an irregular infiltrative process at the orbital apex extending to the cavernous sinus (in THS) or an enlarged lacrimal gland with associated soft-tissue stranding and inflammation (in IgG4-ROD) (5). Patients with IgG4-ROD may have bilateral typically asynchronous lacrimal and salivary gland involvement and orbital myositis, which often lead to proptosis. IgG4-ROD, which accounts for approximately 25% of orbital pseudotumors (40), demonstrates the characteristic findings of IgG4-positive infiltration at biopsy, as well as elevated serum IgG4 levels.

Optic Neuritis

Optic neuritis is an inflammatory demyelinating process of the optic nerve and often manifests clinically as acute and usually painful monocular vision loss, predominantly in female patients with a mean age of 32 years (41) (Fig 22). It is highly associated with multiple sclerosis (Fig 23), occurring in 50% of these patients at some time during the disease course (42). Other cases of optic neuritis have an unknown etiology or are associated with neuromyelitis optica (Fig

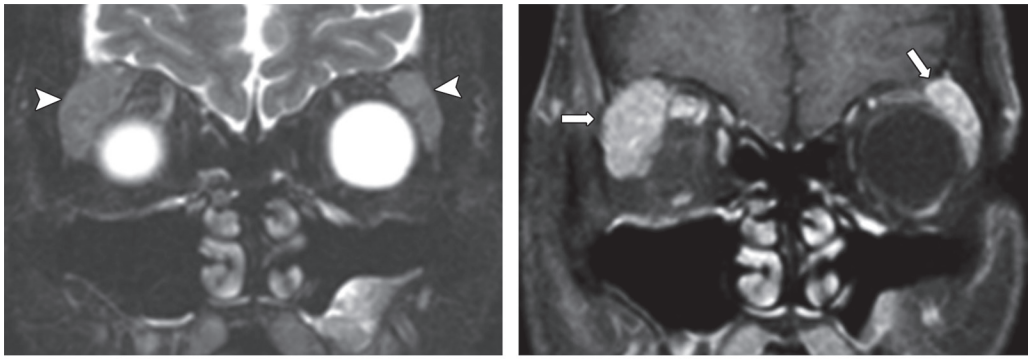

a. b.

Figure 20. IgG4-related orbital disease in a 37-year-old man. **(a)** Coronal T2-weighted MR image shows enlarged lacrimal glands with intermediate signal intensity (arrowheads). **(b)** Coronal contrast-enhanced T1-weighted MR image shows avid enhancement of the lacrimal glands (arrows).

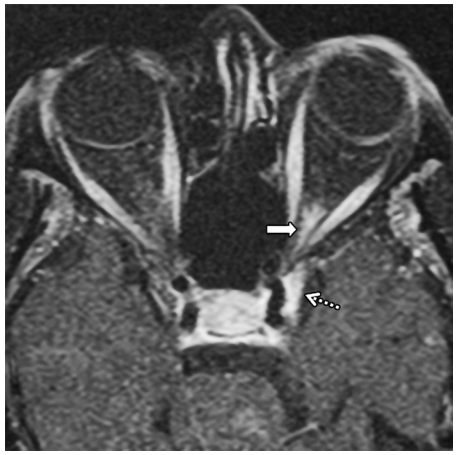

Figure 21. Tolosa-Hunt syndrome in a 47-year-old woman with vision loss and painful ophthalmoplegia. Axial contrast-enhanced fat-saturated T1-weighted MR image through the orbits shows ill-defined enhancement at the left orbital apex (solid arrow) that extends to the cavernous sinus (dotted arrow).

24). Unlike multiple sclerosis, neuromyletis optica affects a slightly older patient population and manifests with more severe clinical attacks of recurrent optic neuritis and long-segment transverse myelitis. Neuromyelitis optica should also be considered in patients with bilateral optic neuritis or severe optic neuritis without spinal cord myelitis (22). The presence of the disease-specific anti–aquaporin-4 antibodies (NMO-IgG or AQP4-Ab) confirms the diagnosis of neuromyletis optica (43).

Postinfectious causes of optic neuropathy should be considered as alternatives to optic neuritis in the pediatric population, while ischemic optic neuropathy (eg, due to vasculopathic risk factors or giant cell arteritis) is a more likely diagnosis than optic neuritis in patients older than 50 years. In general, optic neuritis is a clinical diagnosis that is based on patient history and funduscopic examination. Contrast-enhanced MR imaging of the brain and orbits may increase diagnostic confidence in most cases and provide important information regarding prognosis and treatment response. MR imaging reveals an enlarged enhancing optic nerve with T2-weighted or short inversion time inversion-recovery (STIR) signal hyperintensity relative to that of normal cerebral white matter (22). The longitudinal extent of nerve involvement at MR imaging may correlate with visual impairment at presentation and with the prognosis (44). Visual recovery is often complete and is hastened by use of intravenous corticosteroid therapy.

Conclusion

It is essential for radiologists to recognize characteristic features of orbital emergencies at cross-sectional imaging, especially when clinical evaluation is limited. A systematic approach to assessing orbital emergencies that is based on etiology (infectious, traumatic, vascular, and inflammatory causes) will help craft the appropriate differential diagnosis.

References

1. Channa R, Zafar SN, Canner JK, Haring RS, Schneider EB, Friedman DS. Epidemiology of eye-related emergency department visits. JAMA Ophthalmol 2016;134(3):312–319.
2. Soni NJ, Arntfield R, Kory P. Point-of-care ultrasound. Philadelphia, Pa: Elsevier Saunders, 2014; 252.
3. Modjtahedi BS, Rong A, Bobinski M, McGahan J, Morse LS. Imaging characteristics of intraocular foreign bodies: a comparative study of plain film X-ray, computed tomography, ultrasound, and magnetic resonance imaging. Retina 2015;35(1):95–104.
4. Wippold FJ 2nd; Expert Panel on Neurologic Imaging. Orbits, vision, and visual loss. AJNR Am J Neuroradiol 2010;31(1):196–198.
5. Cunnane ME, Sepahadari AR, Gardiner M, Mafee MF. Pathology of the eye and orbit. In: Som PM, Curtin HD, eds. Head and neck imaging. 5th ed. St Louis, Mo: Elsevier Mosby, 2011; 591–756.
6. Cheng H, Nair G, Walker TA, et al. Structural and functional MRI reveals multiple retinal layers. Proc Natl Acad Sci U S A 2006;103(46):17525–17530.

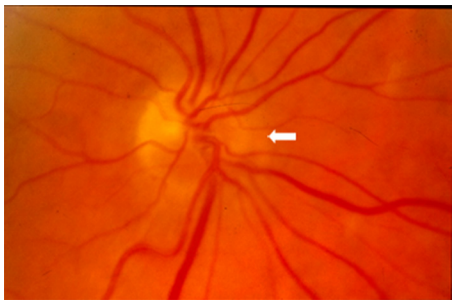

Figure 22. Optic neuritis in a 38-year-old woman. Funduscopic image shows edema of the optic disk with an indistinct margin (arrow).

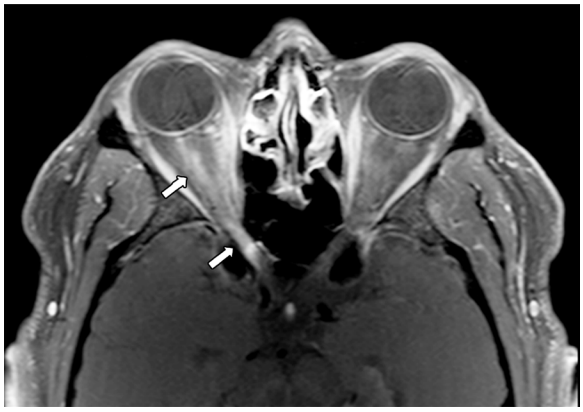

Figure 23. Optic neuritis from multiple sclerosis in a 21-year-old female soccer player with right eye pain and bilateral lower numbness and paresthesia in the lower extremities. Axial contrast-enhanced fat-saturated T1-weighted MR image shows an enlarged enhancing right optic nerve (arrows). This is in contrast to the bilateral optic neuritis in neuromyelitis optica shown in Figure 24.

Figure 24. Optic neuritis with neuromyelitis optica in a 27-year-old woman with bilateral vision loss, left-sided numbness, and positive anti–aquaporin-4 antibodies. Coronal contrast-enhanced fat-saturated T1-weighted MR image through the posterior orbits shows bilateral enlarged enhancing optic nerves with ill-defined margins (arrows). This is in contrast to the unilateral optic neuritis in multiple sclerosis shown in Figure 23.

7. Mafee MF, Som PM. Embryology, anatomy, and imaging of the eye and orbit. In: Som PM, Curtin HD, eds. Head and neck imaging. 5th ed. St Louis, Mo: Elsevier Mosby, 2011; 527–590.
8. Givner LB. Periorbital versus orbital cellulitis. Pediatr Infect Dis J 2002;21(12):1157–1158.
9. Ambati BK, Ambati J, Azar N, Stratton L, Schmidt EV. Periorbital and orbital cellulitis before and after the advent of *Haemophilus influenzae* type B vaccination. Ophthalmology 2000;107(8):1450–1453.
10. Rahbar R, Robson CD, Petersen RA, et al. Management of orbital subperiosteal abscess in children. Arch Otolaryngol Head Neck Surg 2001;127(3):281–286.
11. Ferguson BJ. Mucormycosis of the nose and paranasal sinuses. Otolaryngol Clin North Am 2000;33(2):349–365.
12. Strasser MD, Kennedy RJ, Adam RD. Rhinocerebral mucormycosis: therapy with amphotericin B lipid complex. Arch Intern Med 1996;156(3):337–339.
13. Durand ML. Endophthalmitis. Clin Microbiol Infect 2013;19(3):227–234.
14. Lima V, Burt B, Leibovitch I, Prabhakaran V, Goldberg RA, Selva D. Orbital compartment syndrome: the ophthalmic surgical emergency. Surv Ophthalmol 2009;54(4):441–449.
15. Bhardwaj G, Chowdhury V, Jacobs MB, Moran KT, Martin FJ, Coroneo MT. A systematic review of the diagnostic accuracy of ocular signs in pediatric abusive head trauma. Ophthalmology 2010;117(5):983–992.e17.
16. Kubal WS. Imaging of orbital trauma. RadioGraphics 2008;28(6):1729–1739.
17. Yuan WH, Hsu HC, Cheng HC, et al. CT of globe rupture: analysis and frequency of findings. AJR Am J Roentgenol 2014;202(5):1100–1107.
18. Sung EK, Nadgir RN, Fujita A, et al. Injuries of the globe: what can the radiologist offer? RadioGraphics 2014;34(3):764–776.
19. Nelson LB, Maumenee IH. Ectopia lentis. Surv Ophthalmol 1982;27(3):143–160.
20. Netland KE, Martinez J, LaCour OJ 3rd, Netland PA. Traumatic anterior lens dislocation: a case report. J Emerg Med 1999;17(4):637–639.
21. Boorstein JM, Titelbaum DS, Patel Y, Wong KT, Grossman RI. CT diagnosis of unsuspected traumatic cataracts in patients with complicated eye injuries: significance of attenuation value of the lens. AJR Am J Roentgenol 1995;164(1):181–184.
22. Law M, Lacerda S, Zimmerman R. Anatomy, imaging, and pathology of the visual pathways. In: Som PM, Curtin HD, eds. Head and neck imaging. 5th ed. St Louis, Mo: Elsevier Mosby, 2011; 855–926.
23. Atkins EJ, Newman NJ, Biousse V. Post-traumatic visual loss. Rev Neurol Dis 2008;5(2):73–81.
24. Levin LA, Beck RW, Joseph MP, Seiff S, Kraker R. The treatment of traumatic optic neuropathy: the International Optic Nerve Trauma Study. Ophthalmology 1999;106(7):1268–1277.
25. Chan JW. Traumatic optic neuropathies. In: Chan JW, ed. Optic nerve disorders: diagnosis and management. 2nd ed. New York, NY: Springer, 2014; 155–176.
26. Winegar BA, Murillo H, Tantiwongkosi B. Spectrum of critical imaging findings in complex facial skeletal trauma. RadioGraphics 2013;33(1):3–19.
27. Gruss JS, Hurwitz JJ, Nik NA, Kassel EE. The pattern and incidence of nasolacrimal injury in naso-orbital-ethmoid fractures: the role of delayed assessment and dacryocystorhinostomy. Br J Plast Surg 1985;38(1):116–121.
28. Whitehouse RW, Batterbury M, Jackson A, Noble JL. Prediction of enophthalmos by computed tomography after 'blow out' orbital fracture. Br J Ophthalmol 1994;78(8):618–620.

29. Yamashita K, Noguchi T, Mihara F, et al. An intraorbital wooden foreign body: description of a case and a variety of CT appearances. Emerg Radiol 2007;14(1):41–43.
30. Barrow DL, Spector RH, Braun IF, Landman JA, Tindall SC, Tindall GT. Classification and treatment of spontaneous carotid-cavernous sinus fistulas. J Neurosurg 1985;62(2):248–256.
31. Halbach VV, Hieshima GB, Higashida RT, Reicher M. Carotid cavernous fistulae: indications for urgent treatment. AJR Am J Roentgenol 1987;149(3):587–593.
32. Hayreh SS. Posterior ischaemic optic neuropathy: clinical features, pathogenesis, and management. Eye (Lond) 2004;18(11):1188–1206.
33. Sadda SR, Nee M, Miller NR, Biousse V, Newman NJ, Kouzis A. Clinical spectrum of posterior ischemic optic neuropathy. Am J Ophthalmol 2001;132(5):743–750.
34. Costello F, Kardon RH, Wall M, Kirby P, Ryken T, Lee AG. Papilledema as the presenting manifestation of spinal schwannoma. J Neuroophthalmol 2002;22(3):199–203.
35. Trobe JD. Papilledema: the vexing issues. J Neuroophthalmol 2011;31(2):175–186.
36. Passi N, Degnan AJ, Levy LM. MR imaging of papilledema and visual pathways: effects of increased intracranial pressure and pathophysiologic mechanisms. AJNR Am J Neuroradiol 2013;34(5):919–924.
37. Grassi MA, Lee AG, Kardon R, Nerad JA. A lot of clot. Surv Ophthalmol 2003;48(5):555–561.
38. Lim LH, Scawn RL, Whipple KM, et al. Spontaneous superior ophthalmic vein thrombosis: a rare entity with potentially devastating consequences. Eye (Lond) 2014;28(3):348–351.
39. Mendenhall WM, Lessner AM. Orbital pseudotumor. Am J Clin Oncol 2010;33(3):304–306.
40. Andrew NH, Sladden N, Kearney DJ, Selva D. An analysis of IgG4-related disease (IgG4-RD) among idiopathic orbital inflammations and benign lymphoid hyperplasias using two consensus-based diagnostic criteria for IgG4-RD. Br J Ophthalmol 2015;99(3):376–381.
41. Optic Neuritis Study Group. The clinical profile of optic neuritis: experience of the Optic Neuritis Treatment Trial. Optic Arch Ophthalmol 1991;109(12):1673–1678.
42. Balcer LJ. Clinical practice. Optic neuritis. N Engl J Med 2006;354(12):1273–1280.
43. Martinez-Hernandez E, Sepulveda M, Rostásy K, et al. Antibodies to aquaporin 4, myelin-oligodendrocyte glycoprotein, and the glycine receptor α1 subunit in patients with isolated optic neuritis. JAMA Neurol 2015;72(2):187–193.
44. Hickman SJ, Toosy AT, Miszkiel KA, et al. Visual recovery following acute optic neuritis: a clinical, electrophysiological and magnetic resonance imaging study. J Neurol 2004;251(8):996–1005.